THE JOURNAL OF BIOLOGICAL CHEMISTRY VOL. 289, NO. 50, pp. 34627–34641, December 12, 2014

β-Galactoside α2,6-Sialyltranferase 1 Promotes Transforming Growth Factor-β-mediated Epithelial-Mesenchymal Transition*

Received for publication, July 2, 2014, and in revised form, October 23, 2014 Published, JBC Papers in Press, October 24, 2014, DOI 10.1074/jbc.M114.593392

Jishun Lu[‡], Tomoya Isaji[‡], Sanghun Im[‡], Tomohiko Fukuda[‡], Noritaka Hashii[§], Daisuke Takakura[§], Nana Kawasaki[§], and Jianguo Gu[‡1]

From the [‡]Division of Regulatory Glycobiology, Institute of Molecular Biomembrane and Glycobiology, Tohoku Pharmaceutical University, 4-4-1 Komatsushima, Aobaku, Sendai, Miyagi, 981-8558, Japan and the [§]National Institute of Health Sciences, 1-18-1, Kamiyoga, Setagaya, Tokyo, 158-8501, Japan

Background: Molecular mechanisms underlying the effect of sialylation on tumor progression remain unclear.
Results: ST6GAL1 promoted the TGF-β-induced EMT through down-regulation of E-cadherin-mediated cell adhesion and up-regulation of integrin-mediated cell migration.
Conclusion: Expression of ST6GAL1 is critical for sufficient induction of EMT.
Significance: α2,6-Sialylation of *N*-glycans may play a role in EMT.

β-Galactoside α2,6-sialyltranferase 1 (ST6GAL1) catalyzes the addition of terminal α2,6-sialylation to *N*-glycans. Increased expression of ST6GAL1 has been reported in diverse carcinomas and highly correlates with tumor progression. Here, we report that *St6gal1* transcription and α2,6-sialylated *N*-glycans are up-regulated during TGF-β-induced epithelial-mesenchymal transition (EMT) in GE11 cells, requiring the Sp1 element within the *St6gal1* promoter. Knockdown of *St6gal1* strongly suppressed TGF-β-induced EMT with a concomitant increase in E-cadherin expression, a major determinant of epithelial cell adherens junctions. Conversely, overexpression of ST6GAL1 increased the turnover of cell surface E-cadherin and promoted TGF-β-induced EMT. Overexpressing β-galactoside α2,3-sialyltranferase 4 had little influence on EMT, indicating specificity for α2,6-sialylation. The basal mesenchymal phenotype of MDA-MB-231 human breast cancer cells was partially reversed by ST6GAL1 silencing. Moreover, ST6GAL1 knockdown inhibited the phosphorylation of Akt, but not Smad2, suggesting that ST6GAL1 contributes to EMT through a non-Smad signaling pathway. Taken together, our data indicate that ST6GAL1 promotes TGF-β-dependent EMT as well as maintenance of the mesenchymal state by growth signaling, providing a plausible mechanism whereby up-regulated ST6GAL1 may promote malignant progression.

Epithelial-mesenchymal transition (EMT)[2] is a cellular trans-differentiation process that allows fully polarized epithelial cells to undergo multiple biochemical changes, enabling them to acquire a mesenchymal identity and migrate to secondary sites (1, 2). Morphologically, EMT is characterized by a loss of cell adhesion and acquisition of cell motility. At a molecular level, it is characterized by a decreased expression of cell adhesion molecules and epithelial markers, such as E-cadherin and α3 integrin, and an increased expression of intermediate filament proteins and mesenchymal cell markers, including N-cadherin, α-smooth muscle actin (α-SMA), and vimentin. EMT has evolved as a critical developmental program (3, 4). However, this process is also recapitulated under pathological conditions, prominently in invasion and metastasis of carcinomas (5). A better understanding of the mechanisms involved in EMT is critical to develop efficacious treatments for tumor growth and metastasis.

TGF-β is a pluripotent cytokine and has received much attention as a major inducer of EMT during embryogenesis and cancer progression (6, 7). TGF-β induces EMT through activation of the Smad signaling pathway as well as non-Smad signaling cascades including MAPK/ERK, the Rho family of GTPases, and PI3K/Akt (8, 9). In the Smad-dependent pathway, TGF-β-induced activation of the receptor complex leads to phosphorylation of Smad2 and Smad3 at their C termini by TGF-β receptor I. The phosphorylated Smad proteins then form a trimer with Smad4 and translocate into the nucleus, where they associate and cooperate with other transcription factors to precisely regulate the target gene transcription (10). These reorchestrated target genes, as recently evidenced in several types of cancer cell lines undergoing EMT by mass spectrometry and microarray analysis, at least include the glycogenes involved in *N*-glycosylation, *O*-glycosylation, and sialylation (11–13), indicating the importance of cellular glycosylation pattern in both the transition to and the maintenance of the mesenchymal state.

Sialic acid is the most abundant terminal monosaccharide of glycoconjugates on the eukaryotic cell surface. It is known to be

* This work was supported in part by Grants-in-Aid for Scientific Research 21370059 (to J. G.) and 24570169 (to T. I.) and Grant-in-Aid for Challenging Exploratory Research 23651196 (to J. G.) from the Japan Society for the Promotion of Science, by Scientific Research on Innovative Areas Grants 23110002 (to J. G.) and 23110001 (to N. K.); and the Strategic Research Foundation Grant-aided Project for Private Universities from the Ministry of Education, Culture, Sports, Science and Technology of Japan.
[1] To whom correspondence should be addressed. Tel.: 81-22-727-0216; Fax: 81-22-727-0078; E-mail: jgu@tohoku-pharm.ac.jp.
[2] The abbreviations used are: EMT, epithelial-mesenchymal transition; FN, fibronectin; MAA, *M. amurensis* agglutinin; MET, mesenchymal-epithelial transition; α-SMA, α-smooth muscle actin; SNA, *S. nigra* lectin; ST3GAL4, β-galactoside α2,3-sialyltransferase 4; ST6GAL1, β-galactoside α2,6-sialyltranferase 1; DOX, doxycycline; FT, Fourier transform.

linked via an α2,3 or α2,6 bond to Gal/GalNAc or via an α2,8 bond to sialic acid in proteins through a group of sialyltransferases. Ample evidence demonstrates that sialylation plays fundamental roles in a wide range of normal biological processes, such as cell signaling, differentiation, growth, and apoptosis (14–17). Paradoxically, it has also been shown to contribute to cancer cell progression and metastasis by affecting cell adhesion, migration, and tumor growth (18, 19). Given the essentiality of phenotypic changes in cell adhesion, motility, and growth in EMT, we considered the possible involvement of sialylation in control of EMT.

For this purpose, we investigated the role of sialylation in TGF-β-induced EMT using the normal epithelial cell line, GE11, and mammary cancer cell line, MDA-MB-231 as the EMT and MET (mesenchymal-epithelial transition, the converse process of EMT) models, respectively. Here, we show for the first time that β-galactoside α2,6-sialyltranferase 1 (ST6GAL1), an enzyme that primarily creates terminal α2,6-sialic acid linkages on *N*-glycans, is specifically up-regulated during TGF-β-induced EMT in GE11 cells. Knockdown of *St6gal1* clearly inhibited EMT with a concomitant increase in E-cadherin. Overexpression of ST6GAL1, but not β-galactoside α2,3-sialyltranferase 4 (ST3GAL4) promoted EMT, indicating the specific role of ST6GAL1 during the EMT process. Furthermore, silencing ST6GAL1 partially reversed the basal mesenchymal phenotype of MDA-MB-231 human breast cancer cells. Together, our data show that ST6GAL1 plays a critical role in both the transition to and the maintenance of the mesenchymal state, which provides a plausible explanation for the up-regulated ST6GAL1 during malignant progression of multiple cancers.

EXPERIMENTAL PROCEDURES

Cell Line and Cell Culture—Epithelial GE11 cells, a β1 integrin-null cell line, were kindly gifted by Dr. Arnoud Sonnenberg (Division of Cell Biology, Netherlands Cancer Institute, Amsterdam). The 293T cells were provided from the RIKEN cell bank (Tsukuba, Japan). The phoenix cells and MDA-MB-231 cells were purchased from ATCC. All cells above were cultured in high glucose Dulbecco's modified Eagle's medium (DMEM) with 2 mM L-glutamine and 10% fetal bovine serum (FBS) under a humidified atmosphere containing 5% CO_2 at 37 °C. For the TGF-β-induced EMT model, 5×10^5 cells were plated on 10-cm dishes, followed by incubation with human recombinant TGF-β (PeproTech) at 5 ng/ml for 4 days as described previously (20).

shRNA-mediated Silencing of ST6GAL1 in GE11 Cells and MDA-MB-231 Cells—For the *St6gal1* knockdown in mouse GE11 cells, we utilized the doxycycline (DOX)-inducible shRNA expression system (Invitrogen) as described previously (21). Briefly, the shSt6gal1 targeting sequences (5′-CACCGCGCAAGACAGATGTGTGCTATGTGCTTTAGCACACATCTGTCTTGCGCC-3′ and 5′-AAAAGGCGCAAGACAGATGTGTGCTAAAGCACATAGCACACATCTGTCTTGCGC-3′) were first cloned into the pENTR/H1/TO vector. Then the pENTR/H1/TO-shRNA was recombined into a blasticidin-selectable CS-Rfa-ETBsd, a DOX-inducible shRNA lentiviral vector, by the Gateway™ cloning system (Invitrogen). The resulting vector was then transfected into 293T cells with packaging plasmids by the calcium phosphate for the preparation of viruses. GE11 cells were then infected by the obtained viruses and selected for stable integration with 12.5 μg/ml blasticidin. The shRNA-mediated silencing of *St6gal1* was induced by the addition of 1 μg/ml DOX in the established cell line, and the cells cultured by DOX-free medium were used as the control in the present study. Endogenous *ST6GAL1* in the human MDA-MB-231 cells was knocked down by introducing a shRNA sequence using lentiviral vectors from Sigma-Aldrich. The cells were selected by the addition of 3 μg/ml puromycin.

The Establishment of ST6GAL1- and ST3GAL4-overexpressing GE11 Cells—The previously constructed *ST6GAL1*- or *ST3GAL4*-overexpressing lentiviral vectors (CSIV-TRE-CMV-3xFLAG-*ST6GAL1*/*ST3Gal4*-KT) (21) were transfected into 293T cells with packaging plasmids by the calcium phosphate method for the preparation of viruses. The obtained viruses were then incubated with GE11 cells for 72 h. The infected cells were selected by the Kusabira Orange marker using FACS Aria II (BD Biosciences). The selected cells were transfected with the retrovirus containing the human β1 integrin overexpressed vector (pBABE-puro-β1 integrin). The established cells were further selected by the addition of 3 μg/ml puromycin and used in the present study.

Western Blot Analysis and Immunoprecipitation—Immunoblotting was carried out as described previously (20). Proteins were separated by SDS-PAGE. Samples were incubated at 4 °C overnight with appropriate primary antibodies: anti-E-cadherin (BD Biosciences), anti-N-cadherin (BD Biosciences), anti-α-SMA (Sigma), anti-β1 integrin (BD Biosciences), anti-Smad2 (cell Signaling), anti-phospho-Smad2 (Cell Signaling), anti-Akt (Cell Signaling), anti-phospho-Akt (Cell Signaling), anti-α-tubulin (Sigma), and anti-FLAG (Agilent). Proteins were visualized by chemiluminescence (ECL (Pierce) or Immobilon Western (Millipore)).

Flow Cytometry Analysis of Cells—Cells were grown to about 90% confluence, detached using trypsin containing 1 mM EDTA at 37 °C, and washed three times with cold PBS. Then cells were stained with the 10 μg/ml biotinylated *Sambucus nigra* lectin (SNA), which preferentially recognizes the α2,6-sialylated products or *Maackia amurensis* agglutinin (MAA), which preferentially recognized α2,3-sialylated products for 30 min on ice, followed by incubation with streptavidin-conjugate Alexa Fluor 647 (Invitrogen) for 30 min on ice. Finally, cells were washed three times with PBS and analyzed by flow cytometry (BD Biosciences).

Luciferase Assay—GE11 cells were transiently transfected with a reporter construct derived from basic vector pGL4.10 (Promega), which contained the different *St6gal1* promoters or their truncated fragments or mutated fragments. As an internal control, a *Renilla* luciferase construct (pGL4.82) was co-transfected. Transfected cells were treated with or without TGF-β for 72 h. The cells were lysed and subjected to a luciferase assay using a Dual-Luciferase reporter assay system (Promega) according to the manufacturer's instructions. Primers used to generate the different constructs are listed in Table 1.

N-Glycan Profiling by LC/MS—*N*-Glycan profiling was performed as reported previously (21). Briefly, the same amounts

of cell membrane fractions from GE11 cells treated with or without TGF-β were obtained by an ultracentrifugation and digested with *N*-glycosidase F. The released *N*-glycans were reduced with $NaBH_4$, and the resulting *N*-linked glycans were separated on a graphitized carbon column (Hypercarb, 150 × 0.1 mm, 5 μm; Thermo Fisher Scientific). Mass spectrometric analysis was performed using a Fourier transform ion cyclotron resonance/ion trap type mass spectrometer (FT-MS, LTQ-FT; Thermo Fisher Scientific). The resolution of FT-MS was 50,000, and the scan range was m/z 700–2,000. The monosaccharide compositions of the glycans were deduced from the accurate masses obtained by FT-MS and the product ion spectra.

Cell Surface Biotinylation and Immunoprecipitation—Cell surface biotinylation was performed as described previously (20). Briefly, cells were rinsed twice with ice-cold PBS and were then incubated with ice-cold PBS containing 0.2 mg/ml EZLink Sulfo-NHS-Biotin (Pierce) for 2 h at 4 °C. After incubation, 50 mM Tris-HCl (pH 8.0) was used for the initial wash to quench any unreacted biotinylation reagent. The cells were then washed three times with ice-cold PBS and solubilized in lysis buffer (10 mM Tris-HCl, pH 7.4, 150 mM NaCl, 1% Triton X-100). Insoluble material was removed by centrifugation at 15,000 rpm for 10 min at 4 °C. The supernatant (2 mg of protein) was incubated with streptavidin-agarose (15 μl in 50% slurry) (Upstate Biotechnology, Inc.) for another 3 h at 4 °C with rotation. After washing three times with lysis buffer, the immunoprecipitates were subjected to 7.5% SDS-PAGE, and the separated proteins were transferred to a PVDF membrane. The membrane was incubated with E-cadherin antibody for immunoblot analysis.

Immunofluorescence Staining—Cells cultured on pretreated glass bottom dishes were fixed with acetone/methanol and permeabilized with 0.2% Triton X-100. Antibodies against E-cadherin (BD Bioscience) were used, followed by the incubation with anti-mouse Alexa Fluor 488 secondary antibodies (Invitrogen) and Alexa Fluor 546 phalloidin (Invitrogen) or TO-PRO3 (Invitrogen).

RT-PCR for mRNA Expression Analysis—Total RNA was prepared with TRI reagent (Invitrogen), and 1 μg of total RNA was reverse-transcribed using a PrimeScript RT reagent kit with gDNA Eraser (Takara) according to the manufacturer's instructions. The sequences of the primers used for the PCR amplification were shown in Table 1. The glyceraldehyde-3-phosphate dehydrogenase (GAPDH) mRNA was used as a control in PCR runs, and the reaction products obtained were subjected to electrophoresis using 2% agarose gels containing ethidium bromide.

Cell Migration Assay—Cell Migration was examined with Transwells (BD BioCoat™ control inserts, 8.0-mm inserts; BD Biosciences) as described previously (20). Transwells were coated only on the bottom side with 10 μg/ml fibronectin (FN) at 4 °C overnight. Cells pretreated with or without TGF-β for 4 days were starved in serum-free medium for 12 h, trypsinized, and suspended with 0.5 mg/ml trypsin inhibitor (Nacalai Tesque) in DMEM. The suspended cells were centrifuged, and the supernatants were removed. The resulting cell pellets were resuspended with assay medium (serum-free DMEM) containing TGF-β and diluted to 1×10^5 cells/ml. To each FN-coated transwell, 500-μl aliquots of the cell suspension were added; the cells were then incubated at 37 °C for 4 h. After incubation, cells on the upper side were removed by scraping with a cotton swab. The membranes in the transwells were fixed with 4% paraformaldehyde and stained with 0.5% crystal violet overnight. Cells that had migrated to the lower side were counted using a phase-contrast microscope.

Metabolic Labeling—The pulse-chase experiment was performed as described previously (20). The cells grown at 90% confluence were washed three times with PBS and then starved for 30 min in DMEM without methionine and cysteine (Sigma). After starvation, the cells were pulse-labeled in 500 μl of DMEM containing 200 μCi of [^{35}S]methionine and cysteine (PerkinElmer Life Sciences) for 60 min and then changed with complete DMEM containing 10% FBS at the indicated times. The cells were lysed, and the cell lysates were immunoprecipitated with the anti-E-cadherin antibody and Dynabeads Protein G (Invitrogen). The immunoprecipitates were separated on 4–12% precast gels (Bio-Rad). After drying the gels, radioactive bands were visualized with a Fuji BAS 2500 BioImage analyzer.

Statistical Analysis—Statistical analyses were performed using either a one-tail unpaired Student's t test or one-way analysis of variance, using GraphPad Prism version 5.

RESULTS

St6gal1 and Its Products Were Specifically Up-regulated during the TGF-β-induced EMT in GE11 Cells—Considering the growing evidence for the involvement of sialylation in diverse cellular processes (*e.g.* growth, differentiation, and motility) characteristic of EMT (18, 22), we hypothesized a potential role of cell sialylation in the control of EMT. To test this idea, we initially utilized the established model of EMT, the mouse epithelial cell line, GE11, which undergoes progressive EMT upon TGF-β treatment and acquires a fibroblast-like morphology (20). First, RT-PCR analysis was performed to examine the changes in the expression of glycogenes involved in sialylation biosynthesis during the TGF-β-induced EMT. Interestingly, in contrast to the little difference in the expression of other glycogenes encoding the sialyltransferases, CMP-sialic acid transporter, and neuraminidases, the expression level of ST6GAL1 was significantly up-regulated after stimulation with TGF-β (Fig. 1*A*). These alterations in the expression of glycogenes were further reflected by their enzymatic products analyzed with flow cytometry, as seen in Fig. 1*B*; upon TGF-β treatment, the reactivity against SNA lectin, which specifically recognizes α2,6-sialylation, was greatly increased. In contrast, the reactivity against MAA lectin, which specifically recognizes α2,3-sialylation, showed a marginal change. Consistent with these observations, the complex type of *N*-glycan profiling of those cells by LC/MS showed that the ratios of sialylated *N*-glycans in the TGF-β-treated cells increased obviously, and the opposite asialo-*N*-glycans decreased apparently, when compared with untreated cells (Fig. 1*C*). Taken together, these results clearly demonstrated that *St6gal1* and α2,6-sialylation were specifically up-regulated during the TGF-β-induced EMT process in GE11 cells.

TABLE 1
Primers used for PCR and plasmid construction

	Sense primer (5′–3′)	Antisense primer (5′–3′)
Primers for RT-PCR		
Mouse *St3gal1*	ATGAGGAGGAAGACCCTCAAG	CCACCAGCCTCTTGTTCAAC
Mouse *St3gal2*	GATGAAGTGCTCTCTTCGGG	CAGGCACGATCTGGAACAGT
Mouse *St3gal3*	GTGAAGATGGGACTCTTGGT	ATTGCTCAGGTCGCTGCATG
Mouse *St3gal4*	AGCCATGCTTCCAGGGTGAG	CCTTGAAAGCTACCAGGACC
Mouse *St3gal5*	CTGCCGAGCAATGCCAAGTG	ATCCGGTCAGGGTCCACATA
Mouse *St6gal1*	ATGATTCATACCAACTTGAAG	GGTGCCCCATTAAACCTCAG
Mouse *St6gal2*	CTAGCCAGCAGGTTTTGTCCA	AGCATTCGTTGTCGCCATTG
Mouse *St6galnac1*	CATGACGAGATATTGCAGAGG	CTGCCTTGCTCTGAGGATTC
Mouse *St6galnac2*	AGACCCAGGTTCCCGCCAGG	AAGGAGGTCTTAGTGCCCAC
Mouse *St6galnac3*	ATGGATACATAAATGTGAGGACC	GTGGATACTGTAGCAGGCATCCA
Mouse *St6galnac4*	GTGGTCTACGGGATGGTCAG	GAGAGGCTGAGGCTCAAAGG
Mouse *CST*	AAAGTCGTGGTAGCGCAGAA	ACGTCACAACGATCCCTGAC
Mouse *Neu1*	TTCATCGCCATGAGGAGGTCCA	AAAGGGAATGCCGCTCACTCCA
Mouse *Neu2*	AGGAAGCTACAACGAAGCCACA	TTCTGAGCAGGGTGCAGTTTCC
Mouse *Neu3*	CTCAGTCAGAGATGAGGATGCT	GTGAGACATAGTAGGCATAGGC
Mouse *Neu4*	AGGAGAACGGTGCTCTTCCAGA	GTTCTTGCCAGTGGCGATTTGC
Mouse E-cadherin	CCCAAGCACGTATCAGGGTC	TCTGTGGCGATGATGAGAGC
Mouse N-cadherin	CTGACAATGGAATCCCGCCT	TCCCGCCGTTTCATCCATAC
Mouse α-*SMA*	CTGACAGAGGCACCACTGAA	ATCTCACGCTCGGCAGTAGT
Mouse *Sp1*	ACCATGAGCGACCAAGATCAC	TGGCACCCTGTGAAAGTTGT
Human *ST3GAL1*	GACTTGGAGTGGGTGGTGAG	ACAAGTCCACCTCATCGCAG
Human *ST3GAL2*	CTCTCGGGCAAGAGCTGTG	CTGCAGCATCATCCACCACC
Human *ST3GAL3*	CCTCTCCGCTGTGGTCATTT	GTCCAGCGGAGTCAAAGGAA
Human *ST3GAL4*	TGAGGGTGGCCCGAGG	CCGGGAGTAGTTGCCAAAGA
Human *ST3GAL5*	CCAATGCCAAGTGAGTACACC	TGAGCTCTCTTTACATGGTCAGG
Human *ST3GAL6*	CCACCCCTCACTTTAGCTCC	CAGGTGCCACCCAATAGACA
Human *ST6GAL1*	GAAAAATGGGCCTTGGCCTG	GAGCAGGAAAACAAGCCTGC
Human *ST6GAL2*	TGGGAAGAAGGCTGGTTCATT	TCGTCATCCTCCGGGTAGAA
Human *ST6GALNAC1*	AGCTCAACTACTCCTTGGTGC	CGAAAAGCTTCCTGGGGTCT
Human *ST6GALNAC2*	GCCAGGGACACCACATCATT	GAGGCGATGACTTGGTGAGA
Human *ST6GALNAC3*	AGTTGTGTCCCATACCAGCG	CTGCATGGTCACTCTGTACTGT
Human *ST6GALNAC4*	CATGAAGGCTCCGGGTCGG	CCATGTAGAGCGTGTCTCGG
Human *ST6GALNAC5*	AGGCTCCCAGATTGACCAGA	AGGGTGATTGGGATCCCTGC
Human *ST6GALNAC6*	CAACAAAGAGCAGCGGTCAG	ACAATCACACACTGGTGGCA
Human *CST*	GTGCTCAGGATTTGCAGTTCT	GAGTACCCAGGGCAAAGGTG
Human *Neu1*	TGAGAACGACTTCGGTCTGGTG	CCAGGAAACACCATCATCCTTG
Human *Neu3*	CACCTATGTGGGATCTCCAG	CACCTATGTGGGATCTCCAG
Human *Neu4*	CCGTCTTCCTCTTCTTCATCGC	CATTGCAGTAGAGGAAGCTGCC
Human E-cadherin	ACGCATTGCCACATACA	CGTTAGCCTCGTTCTCA
Mouse α-*SMA*	CCAGCGACCCTAAAGCTTCC	ACCATCACCCCCTGATGTCTG
Human *Sp1*	ACCATGAGCGACCAAGATCA	ATGTTGCCTCCACTTCCTCG
Primers for plasmid construction		
St6gal1-pro-344	TAGGTACCCCGACCAGCATGATGAACTA	CGAAGCTTATGCAGGGAATCTTGCAGTC
St6gal1-pro-625	CTGGTACCACCAGCAATTTTCTGCGTTC	CGAAGCTTAGAGCAAGCAAAACCCAAGA
St6gal1-pro-074	TAGGTACCACCGAGAGAGCACCTCATGT	CGAAGCTTATAGATGCTGAGGGCGAGAA
Pro-344-192	CAAGTCATGGTACCGGCCAGTTAGGCCAGAGAA	CCGGTACCATGACTTGTTTGATCAGGATCACCCT
Pro-344-69	GCCCAAATGGTACCGGCCAGTTAGGCCAGAGAAA	CCGGTACCATTTGGGCTTCCTTGCCTGCCGCATT
Pro-344-33	AAGCCTTTGGTACCGGCCAGTTAGGCCAGAGAAA	CCGGTACCAAAGGCTTGCTCTTTGTGGACAGACT
Pro-344-Sp1-mut	GCTCCGAACCAAAGGCTTGCTCTTTG	CCTTTGGTTCGGAGCAATGCGGCAGGC

The Sp1 Binding Site within St6gal1 Promoter-344 Was Required for Its Transcriptional Activation during TGF-β-induced EMT—The RT-PCR result above showed an enhanced transcription of *St6gal1* in TGF-β-induced EMT. Given the fact that three promoters exist in the mouse *St6gal1* gene, a Dual-Luciferase assay was carried out to determine the core promoter responsible for this enhancement. As shown in Fig. 2*A*, the activity of each promoter increased by 2–3-fold after treatment with TGF-β, indicating that all three promoters were involved in the induction of *St6gal1* expression in EMT. Subsequent sequence analysis of these promoters revealed the presence of several putative Sp1-binding elements and Smad-binding elements in each promoter (Fig. 2*A*). In fact, Sp1 and Smad proteins together have been reported to regulate the expression of vimentin, an important mesenchymal marker involved in cell migration, during TGF-β-induced EMT in pancreatic cancer cells (23). Here, to examine their roles in the regulation of *St6gal1* during the EMT process, we performed a luciferase assay by using the *St6gal1* promoter-344, which assumes highest activity under basal conditions among the three *St6gal1* promoters, and its truncated or mutated constructs as illustrated in Fig. 2*B*. The results showed that upon stimulation by TGF-β, the activity of Smad-binding element-deleted *St6gal1* promoter-344 still increased by ~1.5-fold, albeit it was decreased to some extent as compared with the full-length promoter (~2-fold). However, deleting or mutating the Sp1 elements in *St6gal1* promoter-344 completely abolished its response to TGF-β. These results suggest that the Sp1 element in *St6gal1* promoter-344 is necessary for its transcriptional activation during TGF-β-induced EMT in GE11 cells.

Silencing of St6gal1 Prevented the TGF-β-induced EMT in GE11 Cells—To directly assess the functional contribution of ST6GAL1 in TGF-β-induced EMT, we knocked down the endogenous *St6gal1* by RNA interference technology. Fig. 3*A* showed efficient shRNA-mediated silencing of *St6gal1* in TGF-β-treated GE11 cells. Upon TGF-β stimulation, the morphology of control cells alters from the typical "cobblestone" epithelial cell shape into the diffused fibroblast-like appearance (Fig.

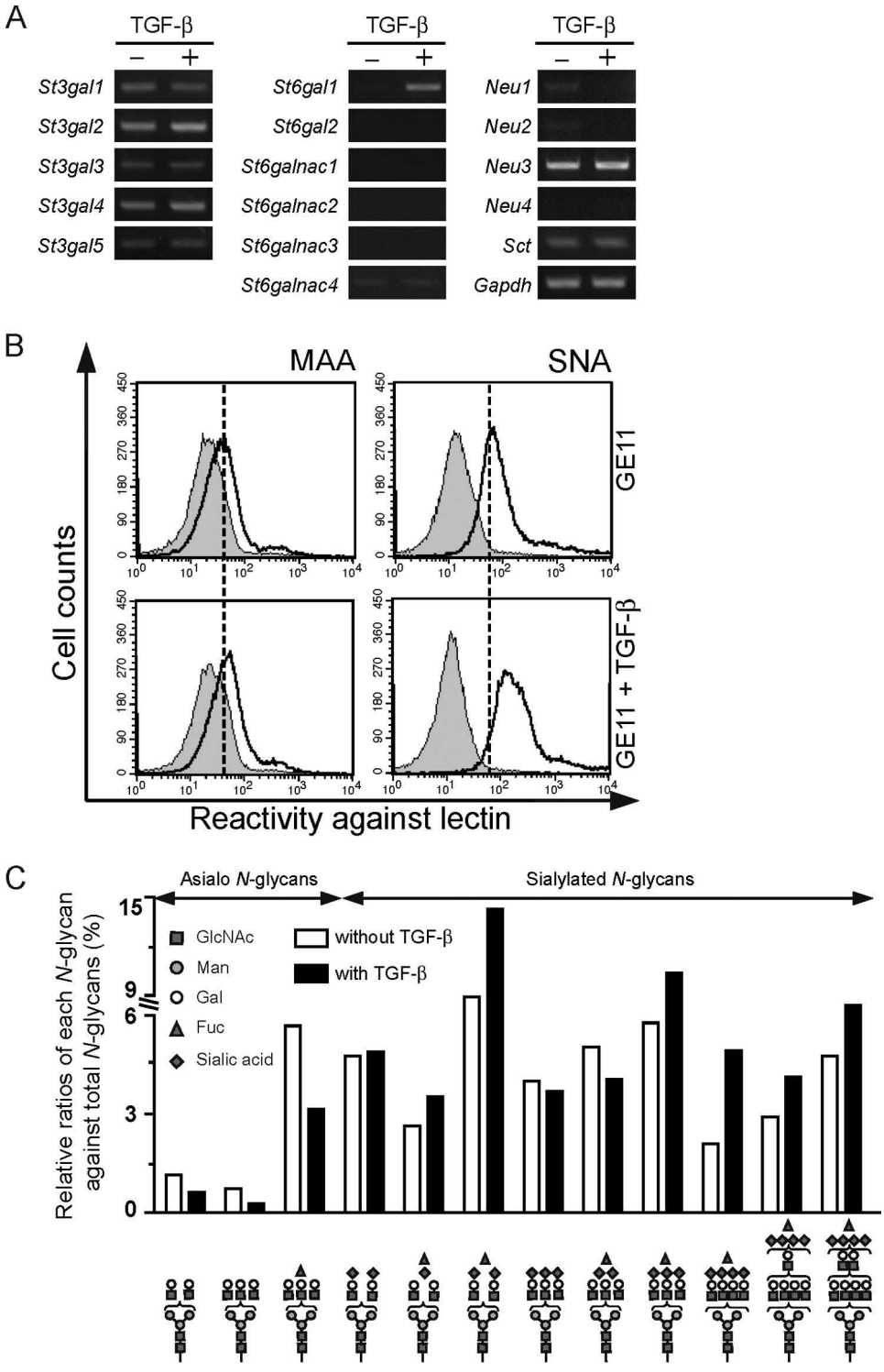

FIGURE 1. ***St6gal1* is specifically up-regulated at the transcriptional level during the TGF-β-induced EMT in GE11 cells.** *A*, RT-PCR using total RNA extracted from TGF-β-treated and -untreated cells was carried out to examine the expression levels of genes involved in protein sialylation. The expression level of *Gapdh* was used as a loading control. *Sct*, sialic acid transporter; *St3gal*, β-galactoside α2,3-sialyltransferase; *ST6Gal*, β-galactoside α2,6-sialyltransferase; *St6galnac*, α-*N*-acetylgalactosaminide α2,6-sialyltransferase; *Neu*, neuraminidase. *B*, cells treated with or without TGF-β were incubated with (*heavy line*) or without (*gray shadow*) biotin-conjugated MAA (recognizing α2,3-sialylated proteins) or biotin-conjugated SNA (recognizing α2,6-sialylated proteins), followed by incubation with streptavidin Alexa Fluor 647 conjugate, and subjected to FACS analysis. *C*, representative glycan profiling in the cells treated with or without TGF-β to compare the major complex type of *N*-glycans by LC/MS. Peak area of asialo- and sialylated *N*-glycans were calculated based on the extracted mass chromatograms acquired in positive and negative modes, respectively. The relative peak area of major *N*-glycans from those cells was presented as a percentage of the total peak area of the glycans. Glycan structures were deduced from the accurate masses and product ion spectra.

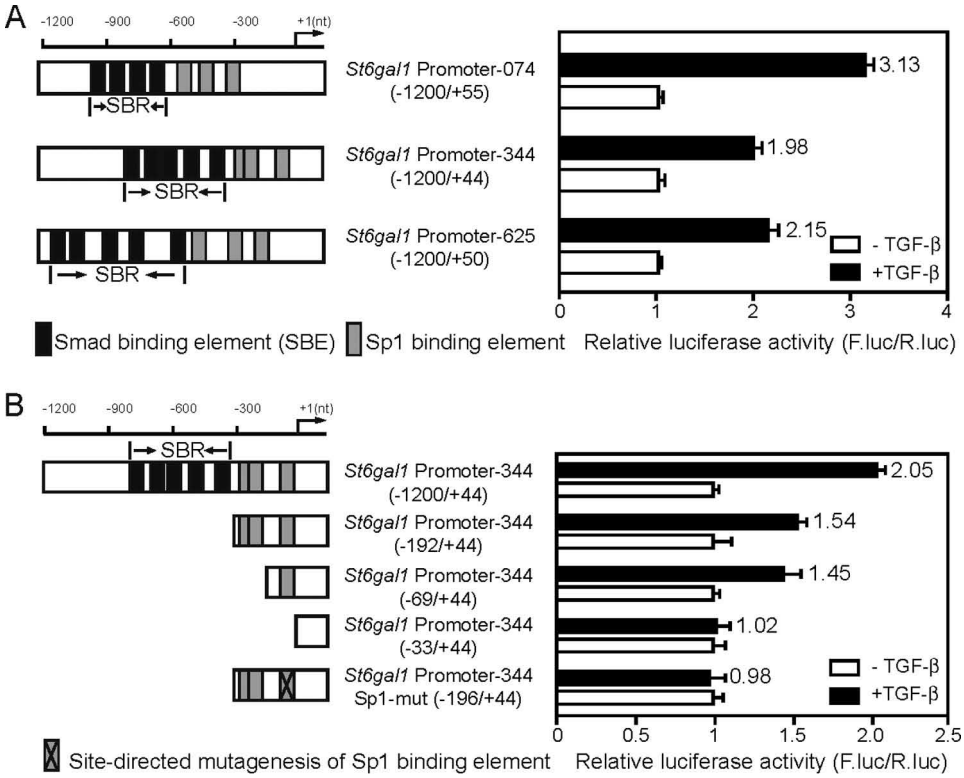

FIGURE 2. **The Sp1 binding site within *St6gal1* promoter-344 is required for its transcriptional activation during TGF-β-induced EMT.** *A* (*left*), representation of three *St6gal1* promoter constructs fused with the luciferase gene, respectively. The relative luciferase activity of each construct is indicated on the *right*. *B* (*left*), representation of the 5′-deleted mutants of *St6gal1* promoter-344 and site-directed mutagenesis of the indicated Sp1 element. The relative luciferase activity of each construct is indicated on the *right*. Each firefly luciferase construct was co-transfected into GE11 cells with a *Renilla* luciferase expression vector as an internal control. Following transfection, luciferase activity was measured after a 72-h incubation with or without TGF-β. The relative luciferase activity was normalized to the luciferase activity of the internal control, which contains the SV40 promoter-enhancer sequences upstream of the luciferase gene. The quantitative data for the relative luciferase activity (*right*) are presented as the means ± S.D. (*error bars*) from three independent experiments. *SBR*, Smad binding region.

3*B*). However, *St6gal1* knockdown cells still displayed a well organized epithelial morphology, indicating a reduced EMT phenotype. In agreement with these morphological changes, shRNA targeting *St6gal1* clearly prevented the loss of epithelial marker E-cadherin and, to a lesser extent, delayed the induction of mesenchymal marker α-SMA (Fig. 3, *C* and *D*). The decelerated loss of E-cadherin after knockdown of *St6gal1* was further confirmed by immunofluorescence analysis (Fig. 3*E*). Although it remains unclear why *St6gal1* knockdown did not affect the expression of N-cadherin, another mesenchymal marker, the results above strongly suggest that *St6gal1* is required for TGF-β-induced EMT. We then asked how *St6gal1* exerted its function in EMT. Considering that TGF-β induces EMT through activation of the Smad signaling pathway as well as non-Smad signaling cascades, including MAP-ERK, the Rho family of GTPases, and PI3K/Akt (8, 9), we first checked the phosphorylation level of Smad2, which acts as a major intracellular effector of Smad signaling. *St6gal1* knockdown did not affect the Smad signaling; as shown in Fig. 3*F*, no significant difference in the expression of phospho-Smad was observed between the *St6gal1* knockdown cells and control cells, indicating that *St6gal1* may contribute to EMT through non-Smad pathways. Given the recent reports showing that *St6gal1* promotes cell migration and invasion by activating PI3K/Akt signaling (21, 24), the activity of this signaling pathway was examined. The phosphorylation level of Akt was clearly decreased after knockdown of *St6gal1* in GE11 cells with or without TGF-β treatment, suggesting that silencing *St6gal1* was able to inhibit the PI3K/Akt signaling in TGF-β-induced EMT.

The Expression of ST6GAL1 Affected the Transcription and Turnover of E-cadherin on Cell Surface—E-cadherin is a transmembrane glycoprotein that plays a crucial role in EMT. Forced expression of E-cadherin has been showed to reverse the EMT in rat kidney fibroblast NRK49f cells (25). Interestingly, here, we found that knockdown of *St6gal1* resulted in an enhancement of E-cadherin transcription (Fig. 4*A*). This up-regulation of E-cadherin was further corroborated by the biotinylation data (Fig. 4*B*) and immunofluorescence staining analysis (Fig. 4, *C* and *D*), where it was seen that *St6gal1* knockdown cells showed a higher level of E-cadherin on the cell surface as compared with the control cells, even after the treatment with TGF-β for 48 h. In addition, considering the growing evidence for the involvement of ST6GAL1 in the cell surface retention of glycoproteins (26, 27), we were wondering whether this is also true for the E-cadherin in GE11 cells. To verify this, the pulse-chase experiment was performed using the ST6GAL1-overexpressing cells. As shown in Fig. 4, *E* and *F*, the decay rate of E-cadherin was increased after overexpression of ST6GAL1 in GE11 cells. The results above indicate that the increased expression of E-cadherin on the surface of *St6gal1* knockdown cells is due not only to its up-regulated transcription but also to its prolonged turnover.

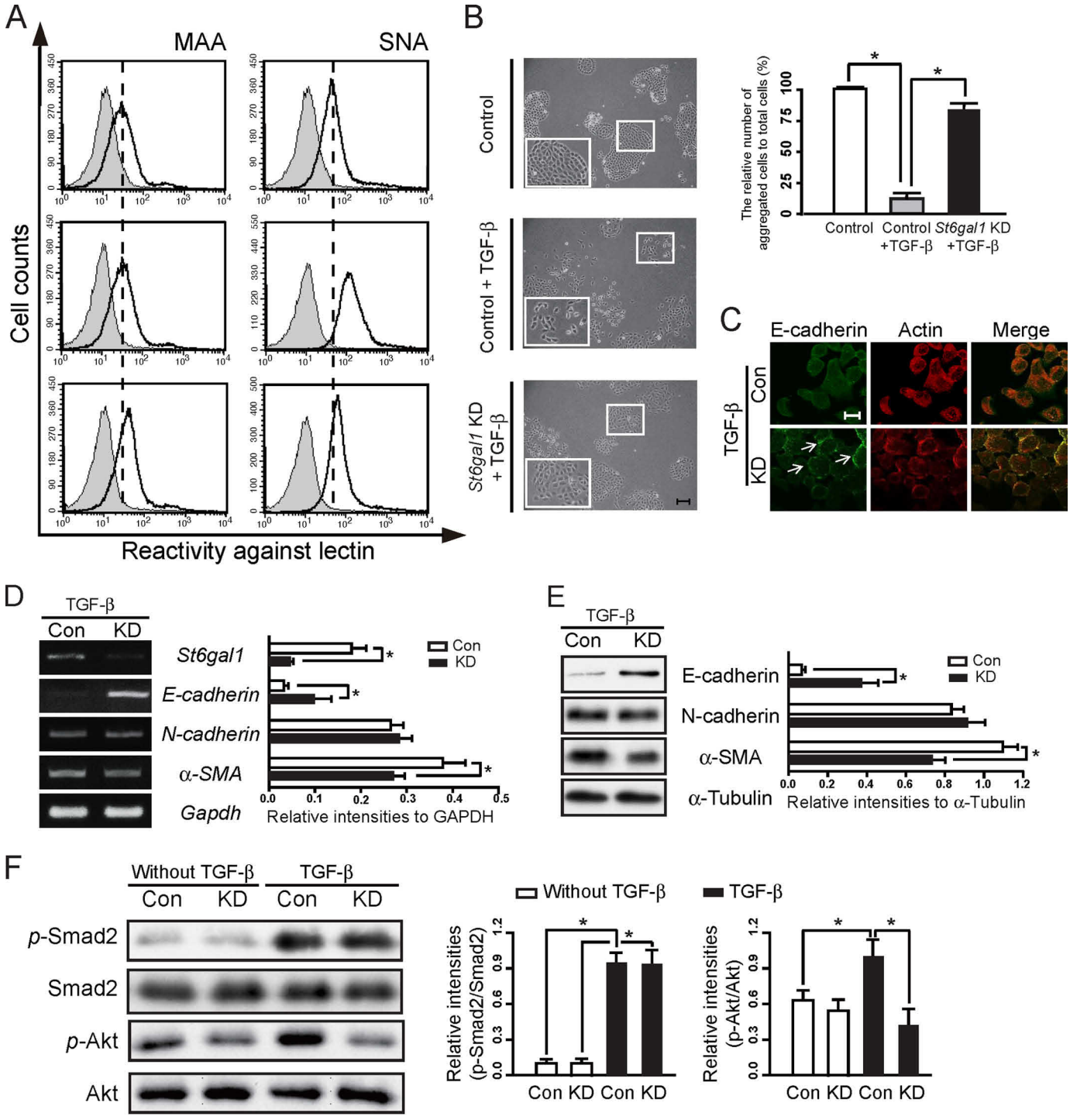

FIGURE 3. **Silencing of *St6gal1* prevents the EMT-associated morphological and molecular changes upon TGF-β stimulation in GE11 cells.** DOX-inducible shRNA-*St6gal1* GE11 cells were grown with or without DOX for 24 h and were then treated with TGF-β and incubated for another 72 h. *A*, the cells were collected and incubated with (*heavy line*) or without (*gray shadow*) biotin-conjugated SNA or biotin-conjugated MAA, followed by incubation with streptavidin Alexa Fluor 647 conjugate and subjected to FACS analysis to confirm the *St6gal1* knockdown efficiency. *B*, bright field pictures were taken to show the cell morphology. *Insets*, a representative cell morphology and its magnified view. *Scale bar*, 100 μm. The quantitative data for the number of aggregated cells relative to the total cells are presented as means ± S.D. (*error bars*) from three independent experiments (*, $p < 0.01$ by one-tailed unpaired Student's *t* test). *C*, to visualize the effects of *St6gal1* knockdown on the E-cadherin on cell surface, the indicated cells stimulated by TGF-β were stained with anti-E-cadherin antibody, followed by the incubation with fluorescent secondary antibody. Localization of F-actin was examined by staining with Alexa Fluor 546 phalloidin. *Scale bar*, 50 μm. The *arrows* indicate the E-cadherin expressed in the cell-cell contact. *D*, RT-PCR using total RNA extracted from those cells was carried out to examine the expression levels of E-cadherin, N-cadherin, and α-SMA. The expression level of *Gapdh* was used as a loading control. The quantitative data are presented as the means ± S.D. from three independent experiments (*, $p < 0.01$ by one-tailed unpaired Student's *t* test). *E*, cell lysates from those cells were immunoblotted with anti-E-cadherin, anti-N-cadherin, and anti-α-SMA antibodies. α-Tubulin was used as a loading control. The quantitative data are presented as the means ± S.D. from three independent experiments (*, $p < 0.01$ by one-tailed unpaired Student's *t* test). *F*, the indicated cell lysates were immunoblotted by phospho-Smad2, Smad2, phospho-Akt, and Akt antibodies. α-Tubulin was used as a loading control. The quantitative data are presented as means ± S.D. from three independent experiments (*, $p < 0.01$ by one-tailed unpaired Student's *t* test). *Con*, DOX-inducible shRNA-*St6gal1* GE11 cells; *St6gal1 KD*, DOX-inducible shRNA-*St6gal1* GE11 cells induced by DOX.

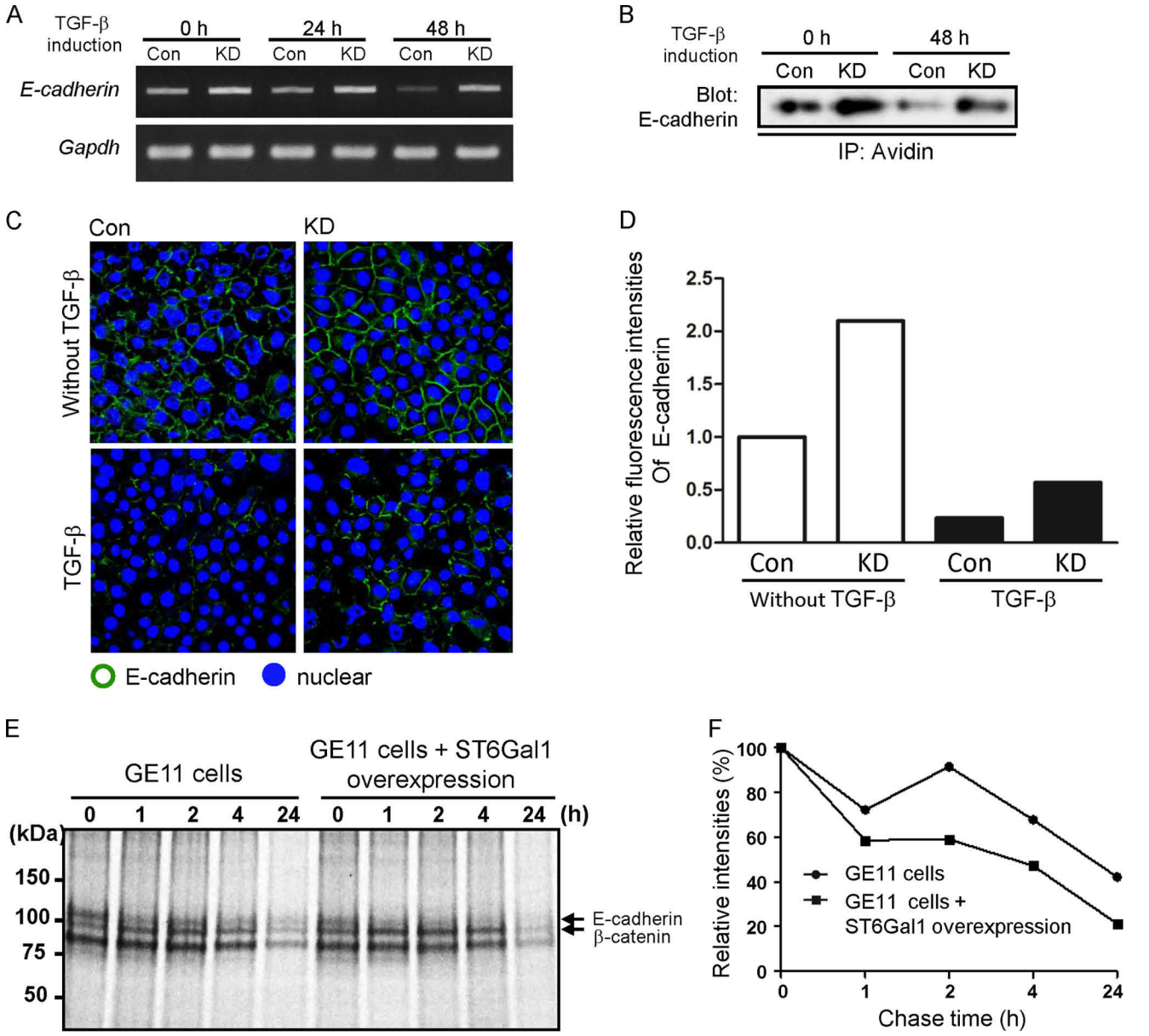

FIGURE 4. **The expression of ST6GAL1 affected the transcription and turnover of E-cadherin on the cell surface.** DOX-inducible shRNA-*St6gal1* GE11 cells were grown with or without DOX for 24 h and were then treated with TGF-β and incubated for another 48 h. *A*, time course analysis of the E-cadherin expression in cells treated with TGF-β for 0, 24, and 48 h by RT-PCR. The expression level of *Gapdh* was used as a loading control. *B*, cell surface biotinylation was performed as described under "Experimental Procedures." Equal amounts of the cell lysates were immunoprecipitated with avidin-agarose and immunoblotted with anti-E-cadherin antibody to examine the level of cell surface E-cadherin in the indicated cells. *C*, to directly visualize the effects of *St6gal1* knockdown on the E-cadherin on the cell surface, the indicated cells treated with or without TGF-β were stained with anti-E-cadherin primary antibody, followed by the incubation with fluorescent secondary antibody and TO-PRO-3. *D*, the relative fluorescence intensities of E-cadherin were quantified by the software ImageJ. *E*, the pulse-chase experiment was performed as described under "Experimental Procedures." The same amounts of the cell lysates were immunoprecipitated with anti-E-cadherin antibody at the indicated times. *F*, the relative E-cadherin intensities at each chasing point were quantified by the software ImageJ. The intensities of E-cadherin at the 0 h point of the ST6GAL1 overexpressed cells and control cells were set as 100%, respectively.

Overexpression of ST6GAL1, but Not ST3GAL4, Promoted the TGF-β-induced EMT—Although repression of ST6GAL1 activity by shRNA inhibited TGF-β-induced EMT, the influence could be due to potential off-target effects of the designed sequence. To rule out this possibility, we established a ST6GAL1-expressing GE11 cell line. The expression level of ST6GAL1 was verified by immunoblot analysis, and its enzymatic products were examined by FACS analysis (Fig. 5*A*). To evaluate the effects of the ST6GAL1 overexpression on TGF-β-induced EMT, RT-PCR (Fig. 5*C*) and Western blot (Fig. 5*D*) analyses were performed. The results showed that forced expression of ST6GAL1 promoted the loss of epithelial marker E-cadherin and accelerated the induction of mesenchymal marker α-SMA. Similar to the *St6gal1* knockdown cells, ST6GAL1-overexpressing cells exhibited no significant difference in the expression of N-cadherin from control cells. These results further corroborate that ST6GAL1 is required for the TGF-β-induced EMT in GE11 cells. ST6GAL1 mainly catalyzes the terminal α2,6-sialylation on *N*-glycans. This prompted us to ask whether α2,3-sialylation of *N*-glycans also plays a critical role in EMT. To address this question, we overexpressed ST3GAL4, which is primarily responsible for the α2,3-sialyla-

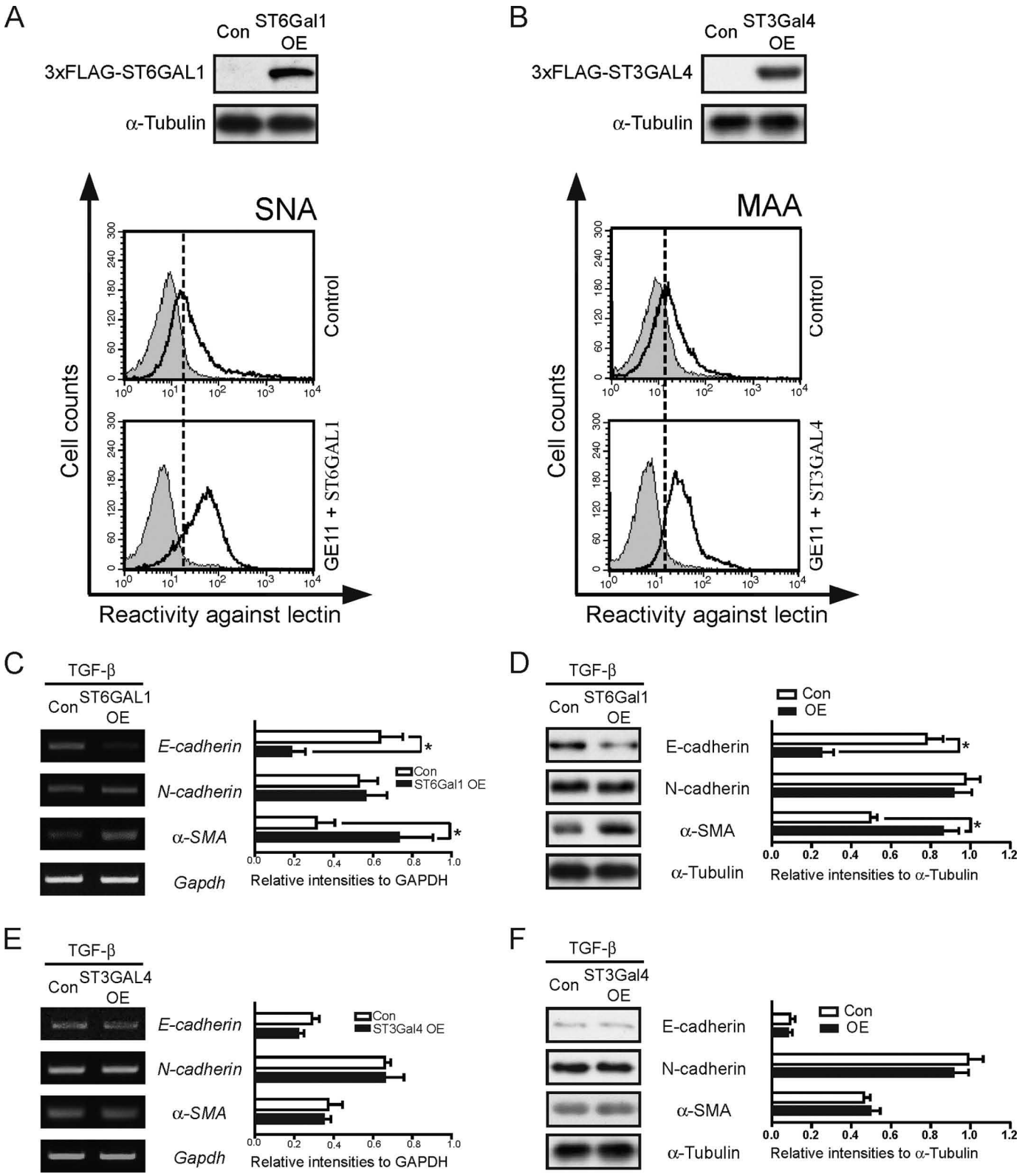

FIGURE 5. **Forced expression of ST6GAL1, but not ST3GAL4, promotes the EMT-associated molecular changes upon TGF-β stimulation in GE11 cells.** DOX-inducible *3xFLAG-ST6GAL1*- or *3xFLAG-ST3GAL4*-overexpressing GE11 cells were treated with or without 1 μg/ml DOX for 24 h, followed by the addition of TGF-β for another 48-h incubation. The expression level of *ST6GAL1* (*A*) and *ST3GAL4* (*B*) was confirmed by Western blot analysis using anti-FLAG antibody, and their enzymatic products were examined by FACS analyses using lectins, as described under "Experimental Procedures." *C* and *E*, RT-PCR analysis using the total RNA extracted from those cells was carried out to examine the expression levels of E-cadherin, N-cadherin, and α-*SMA*. The expression level of *Gapdh* was used as a loading control. The quantitative data are presented as means ± S.D. (*error bars*) from three independent experiments (*, $p < 0.01$ by one-tailed unpaired Student's *t* test). *D* and *F*, cell lysates from those cells were immunoblotted with anti-E-cadherin, anti-N-cadherin, and anti-α-SMA antibodies. α-Tubulin was used as a loading control. The quantitative data are presented as means ± S.D. from three independent experiments (*, $p < 0.01$ by one-tailed unpaired Student's *t* test).

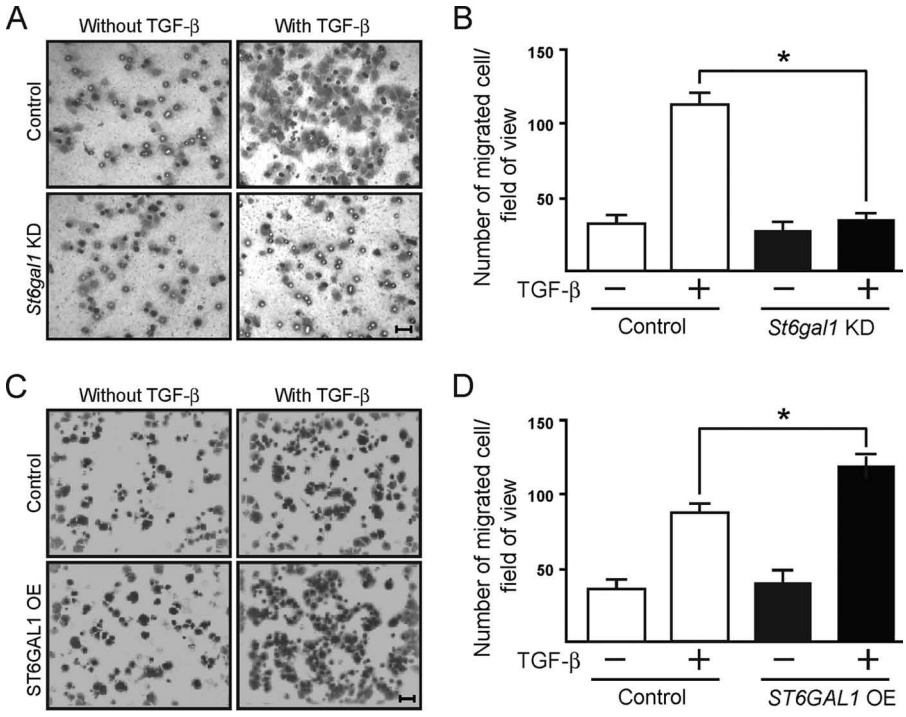

FIGURE 6. **Knockdown of *St6gal1* almost completely abrogates the TGF-β-induced cell migration, whereas the induction of TGF-β-mediated migration is significantly accelerated after overexpression of *ST6GAL1*.** The migratory ability of *St6gal1* knockdown cells (*A* and *B*) and *ST6GAL1*-overexpressing cells (*C* and *D*) toward FN was determined by a transwell assay. Cells that migrated through the transwell membrane were stained with 0.5% crystal violet. *A* and *C*, representative example recorded by phase-contrast microscopy. *Scale bar*, 100 μm. *B* and *D*, the migrated cells were counted under a microscope. The quantitative data were obtained from three independent experiments. The *p* values were calculated using one-tailed unpaired Student's *t* test. *Error bars*, S.D. *, $p < 0.01$.

tion of *N*-glycans, and replicated the experiments above. Fig. 5*B* showed the successful overexpression of ST3GAL4 and increased α2,3-sialylated products in GE11 cells. Subsequent RT-PCR (Fig. 5*E*) and Western blot (Fig. 5*F*) analyses indicated that there was little difference in the expression of EMT-associated molecules between ST3Gal4-overexpressing cells and control cells, highlighting the specific role of ST6GAL1 in control of EMT.

ST6GAL1 Was Required for the Cell Migration in TGF-β-induced EMT—A phenotypic hallmark of EMT is the stimulation of cell migration. Therefore, we assessed the migratory ability of GE11 cells by transwell analysis. As shown in Fig. 6, GE11 cells become highly migratory upon treatment with TGF-β. However, repression of ST6GAL1 expression significantly prevented TGF-β-induced increase in cell migration (Fig. 6, *A* and *B*). Conversely, overexpression of ST6GAL1 accelerated the induction of the TGF-β-mediated cell migration. These results indicated that ST6GAL1 is required for the enhancement of the cell migration during TGF-β-induced EMT.

ST6GAL1 Knockdown Induced MET-like Phenotypes in a Breast Cancer Cell Line—EMT illustrates the differentiation plasticity during the normal development and pathological process and is complemented by a reverse process called MET. To define the role of ST6GAL1 in MET, we knocked down endogenous *ST6GAL1* by RNA interference in the aggressive mesenchymal breast cancer cell line MDA-MB-231. Fig. 7, *A* and *B*, showed the successful silencing of *ST6GAL1* in this cell line. According to RT-PCR (Fig. 7*B*) and Western blot (Fig. 7*C*) analyses, we found that knockdown of *ST6GAL1* led to an increase in E-cadherin expression while decreasing the expression levels of the mesenchymal markers, such as α-SMA, β1 integrin, and FN. Furthermore, consistent with this reduced EMT, as shown at the expression level, repression of *ST6GAL1* activity significantly decreased the ability of MDA-MB-231 cells to migrate through the transwell membrane when compared with control cells (Fig. 7, *D* and *E*). These effects of ST6GAL1 knockdown on EMT in MDA-MB-231 cells, as in GE11 cells, were mediated via a non-Smad signaling pathway, because little difference in the expression level of phospho-Smad2 was observed between knockdown cells and control cells (Fig. 7*F*). Taken together, the results above suggest that the expression of ST6GAL1 plays an important role in EMT.

DISCUSSION

EMT is a cellular transdifferentiation process that plays critical roles in embryonic development and metastasis formation during malignant progression. The mechanisms underlying EMT have been extensively explored in the past decade. A vast amount of knowledge has been obtained from the research examining EMT at the mRNA and protein level. In the present study, we investigated the role of sialylation, a post-translational modification, in TGF-β-induced EMT and showed that ST6GAL1-mediated α2,6-sialylation is required for the sufficient induction of TGF-β-mediated EMT. In particular, we show here that *St6gal1* was specifically up-regulated during the TGF-β-induced EMT process in GE11 cells. Knockdown of *St6gal1*, interestingly, enhanced the transcription of E-cad-

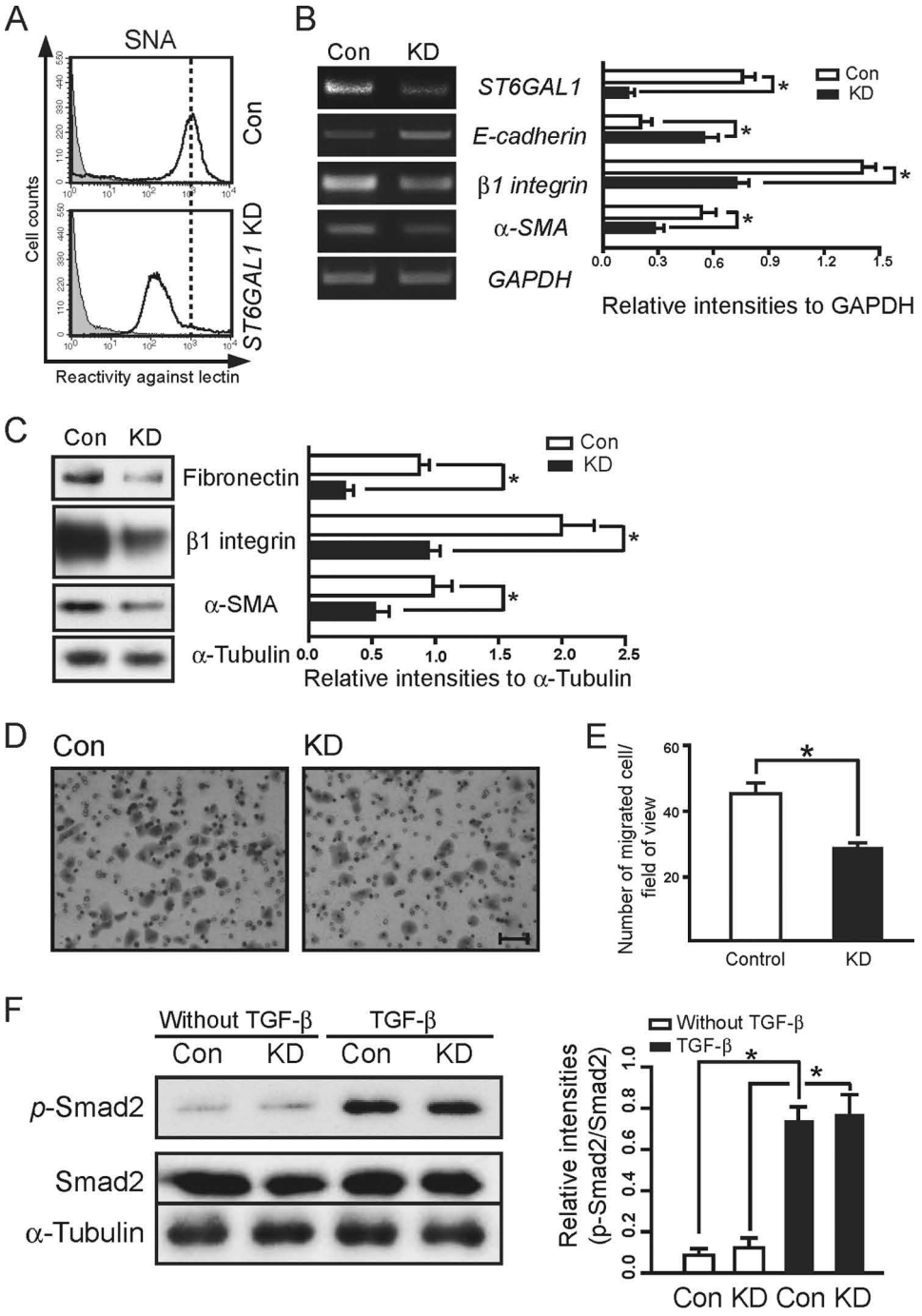

FIGURE 7. **Silencing *ST6GAL1* partially reverses the basal mesenchymal phenotype of MDA-MB-231 cells.** *A*, the indicated cells were collected and incubated with (*heavy line*) or without (*gray shadow*) biotin-conjugated SNA, followed by incubation with streptavidin Alexa Fluor 647 conjugate and subjected to FACS analysis to check the *St6gal1* knockdown efficiency. *B*, RT-PCR was carried out to examine the expression levels of *ST6GAL1*, E-cadherin, β1 integrin, and *α-SMA* in the indicated cells. The expression level of *GAPDH* was used as a loading control. The quantitative data are presented as means ± S.D. from three independent experiments (*, $p < 0.01$ by one-tailed unpaired Student's *t* test). *C*, cell lysates from those cells were immunoblotted (*IB*) with anti-fibronectin, anti-β1 integrin, and anti-α-SMA antibodies. α-Tubulin was used as a loading control. The quantitative data are presented as means ± S.D. from three independent experiments (*, $p < 0.01$ by one-tailed unpaired Student's *t* test). *D*, cell migration toward FN was determined by a transwell assay. A representative example was recorded by phase-contrast microscopy. *Scale bar*, 100 μm. *E*, the migrated cells were counted under a microscope. The quantitative data were obtained from three independent experiments. The *p* values were calculated using a one-tailed unpaired Student's *t* test. *Error bars*, S.D. *, $p < 0.01$. *F*, the indicated cell lysates was immunoblotted by anti-phospho-Smad2 and anti-Smad2 antibodies. α-Tubulin was used as a loading control. The quantitative data are presented as the means ± S.D. from three independent experiments (*, $p < 0.01$ by one-tailed unpaired Student's *t* test).

herin and strongly suppressed TGF-β-induced EMT, as evidenced not only by a prevention of the EMT-associated morphological and molecular changes but also by an inhibition of the TGF-β-mediated stimulation of cell migration. On the other hand, by using the MDA-MB-231 cells as a MET model, we observed that silencing *ST6GAL1* repressed the mesenchymal properties of this aggressive human breast cancer cell line and normalized these cells to an epithelial phenotype, indicating that ST6GAL1 is also important for maintenance of the cell mesenchymal state.

Our findings here that silencing of ST6GAL1 significantly inhibited the TGF-β-induced cell migration in GE11 cells as well as MDA-MB-231 cells indicate an important role of ST6GAL1 in the stimulation of cell migration. In line with our observations, much of the literature showed that ST6GAL1 promotes cell migration and invasion during cancer progression (28, 29). The function of ST6GAL1 in promoting cell migration might be partially mediated through affecting galectin-involved signalings because galectin-3 is highly correlated with cancer malignancy by regulating various biological processes (30, 31), and α2,6-sialylation of β1 integrin could impair their interaction with galectin-3, thereby facilitating cell migration (32). On the other hand, accumulating evidence suggested that ST6GAL1 renders the cells resistant to apoptosis. Bellis's group clearly demonstrated that ST6GAL1 serves as a major inhibitor of cell death pathways initiated by Fas, TNFR1, and galectins (14, 15, 33). Additionally, ST6GAL1 has also been shown to confer radiation resistance in colon cancer cell lines (34) as well as multidrug resistance in human acute myeloid leukemia (35). These studies imply that up-regulation of ST6GAL1 in TGF-β-induced EMT may also reduce the apoptosis sensitivity in response to various stimuli, thus extending the cell life span. Clearly, further investigation is needed to support this potential role of ST6GAL1 in EMT.

It is well known that E-cadherin is a major determinant for maintenance of the cell epithelial integrity and plays a crucial role in EMT. Loss of E-cadherin was sufficient to convert A549 NSCLC cells into the mesenchymal type (36). Conversely, forced expression of E-cadherin reversed the EMT in rat kidney fibroblast NRK49f cells (25). Here, we show that knockdown of ST6GAL1 up-regulated the transcription of E-cadherin, and overexpression of ST6GAL1 decreased the retention of cell surface E-cadherin, which provide a possible mechanism by which ST6GAL1 functions in EMT. Although it is difficult to give a plausible explanation for the up-regulated transcription of E-cadherin in ST6GAL1 knockdown cells based on the previous studies, the reduced retention of cell surface E-cadherin in ST6GAL1-overexpressing cells could be caused by the increased α2,6-sialylation of E-cadherin because growing evidence has shown that ST6GAL1 is involved in the cell surface retention of glycoproteins and E-cadherin is its direct substrate (26, 27). On the other hand, TGF-β triggers EMT mainly via the Smad signaling pathway. However, our data show that *St6gal1* knockdown did not affect this major TGF-β-Smad signaling. Instead, it inhibited the activity of the PI3K/Akt signaling cascade. In fact, activation of PI3K/Akt signaling plays a crucial complementary role in elaboration of the EMT process (37, 38). Treatment of cells with chemical inhibitors that selectively or specifically block this pathway dramatically affects the induction of the EMT phenotype. Accordingly, it can be concluded that the effects of ST6GAL1 on EMT induction and cell migration were also mediated through the PI3K/Akt signaling pathway. In agreement with this, several groups, including us, recently reported that ST6GAL1 promotes cell migration and invasion by activating PI3K/Akt signaling (21, 24), and this enhanced migratory response has been shown to be due, at least in part, to ST6GAL1-mediated sialylation of the β1 integrin receptor (19, 39, 40). Nonetheless, the GE11 cell utilized here is a β1 integrin-null cell line. This implies that there exist additional mediator proteins for promoting the cell migratory ability in TGF-β-induced EMT. Given the finding here that *St6gal1* knockdown reduced the fibronectin-mediated cell migration upon TGF-β stimulation, the candidate mediator may exist in fibronectin receptors. Besides $\alpha5\beta1$ integrin, $\alpha v\beta3$ and $\alpha v\beta6$ serve as the important receptors for fibronectin as well, and both of them are deeply implicated in the promotion of cancer cell metastasis (41–44). Considering also a growing body of evidence for the cross-talk between αv integrins and TGF-β during EMT (45), it is reasonable to speculate that ST6GAL1 may affect the PI3K/Akt signaling pathway by modulating the sialylation status of αv integrin in GE11 cells. Meanwhile, apart from αv integrin, we could not rule out the possibility of the existence of additional mediators like receptor tyrosine kinases that participate in the PI3K/Akt or other non-Smad signaling transduction, because it has been shown that desialylation of insulin-like growth factor receptor quenches the Akt- and ERK-involved signaling in response to insulin-like growth factor II (46), and recently, overexpression of NEU1, which accounts for 70% of the sialidase activity of epithelial cells, diminished epidermal growth factor (EGF)-stimulated autophosphorylation of EGF receptor (47). Further investigation is obviously needed to elucidate the mechanistic roles of ST6Gal in TGF-β-induced EMT in more detail.

EMT is a complex and multifaceted process that requires a precise regulation of gene expression. Mounting evidence showed that this well orchestrated gene expression in EMT is achieved by the cooperative actions of a number of transcription factors. It has been shown, for instance, that transcription factors Sp1 and Smad form transcriptional complexes at the promoter binding region of vimentin and together regulate the expression of this critical EMT-associated protein (23). Likewise, we find that Sp1 and Smad proteins were also involved in the specific up-regulation of *St6gal1* during TGF-β-induced EMT. However, in contrast to the case of vimentin, in which Sp1 and Smad together act as a switch for vimentin expression, these two transcription factors may function to regulate the *St6gal1* expression independently, because deletion of the putative Smad binding sites within the *St6gal1* promoter only decreased the efficiency of *St6gal1* induction instead of completely abrogating its promoter activity. Recently, Sp1 and Smad proteins have been found to control the expression of tumor suppressor NDRG2 in a similar way during the TGF-β-induced EMT (48). These observations raise the question of how this regulatory strategy of *St6gal1/NDRG2* expression benefits the cells. One possible advantage is that it may favor the precise tuning and regulation of *St6gal1*/*NDRG2* levels to meet the requirements in different biological scenarios that they participate in. In agreement with this idea, Sp1 elements, but not together with Smad elements, within the human *ST6GAL1* promoter have been shown to be important for efficient transcription of *ST6GAL1* during the HL-60 cell differentiation induced by dimethyl sulfoxide (49). A detailed characterization of the *St6gal1* promoter in a different biological context is required for better understanding of its regulatory mechanisms.

In addition to *St6gal1*, we have previously reported that TGF-β also down-regulates the expression of *N*-acetylglucos-

aminyltransferase III (*Mgat3*), which is responsible for the synthesis of a bisecting *N*-acetylglucosamine (GlcNAc) in *N*-glycan, and up-regulates the expression of *N*-acetylglucosaminyltransferase V (*Mgat5*), which catalyzes the β1,6-GlcNAc branching in *N*-glycan in EMT (20). In fact, the introduction of a bisecting GlcNAc suppresses β1,6-GlcNAc branching formation because MGAT5 cannot utilize the bisected oligosaccharide as an acceptor (50–52), indicating the coordinated regulation of gene expression during EMT. Therefore, given the concomitant enhancement of ST6GAL1 in EMT, it is conceivable that the *N*-glycan structure remodeled by altered expression of MGAT3 and MGAT5 may facilitate (or at least not inhibit) the subsequent ST6GAL1-mediated sialylation. Consistent with this idea, Pinho *et al.* (53) reported that E-cadherin undergoes extensive modification of *N*-glycans with enhanced β1,6-GlcNAc branching and α2,6-sialylation during acquisition of the malignant phenotype in a canine mammary tumor cell line. Additionally, the increase in β1,6-GlcNAc branching and α2,6-sialylation in the mouse serum glycome has been shown to correlate with inflammation and ovarian tumor progression (54). In the past decade, growing evidence has shown that both ST6GAL1 and MGAT5 promote cell migration and invasion (19, 55). Based on the hypothesis above, it is highly possible that the enhanced migratory response of those cells with high expression of ST6GAL1 as well as MGAT5 is due, at least mainly, to the up-regulated α2,6-sialylation, and MGAT5 may act as an important coordinator for a better ST6GAL1-mediated sialylation. In agreement with this corollary hypothesis, we find here that despite the enhancement of MGAT5 expression in EMT in GE11 cells (data not shown), silencing of *St6gal1* almost completely inhibited the increased migratory ability upon TGF-β stimulation. Furthermore, this idea is further supported by a recent study (56) indicating that ST6GAL1 is responsible for the different invasive properties in the murine hepatocarcinoma Hca-F (high metastatic potential) and Hca-P (low metastatic potential) cells, although both *St6gal1* and *Gnt-V* are highly expressed in Hca-F cells as compared with in Hca-P cells.

It is worth noting that overexpression of ST6GAL1, but not ST3GAL4, was found to promote the TGF-β-induced EMT, although both of them catalyze the sialylation of *N*-glycan. This discrepancy in their function in EMT may be attributed to their different effects on the specific glycoproteins. As examples, α2,6-sialylation alters (i) the conformation of β1 integrin (57); (ii) clustering of CD45 (58), EGF receptor (59), and PECAM (27); and (iii) cell surface retention of PECAM (27) and the Fas death receptor (14), whereas little literature showed the involvement of ST3GAL4 in those aspects. Given that both of ST6GAL1 and ST3GAL4 create the sialylation with similar sugar size and negative charge on *N*-glycans, it is tempting to speculate that their different effects on the given glycoprotein may result from the different localization of the sialic acids that they add within the glycoprotein tertiary structure. Although it is difficult to determine due to technical challenges, a comparison of the crystal structure of the ST6GAL1 and ST3GAL1 revealed a significant difference in their glycan acceptor binding regions (60), which provides indirect evidence for the hypothesis above.

Recently, high expression of ST6GAL1 has also been identified in induced pluripotent stem cells and cancer stem cells and correlates with stem cell markers in normal tissues and colon cancer cell lines (61). Considering the emerging evidence that the EMT program may give rise to cancer stem cells or at least cells with stem cell-like properties (62), our research here provides further support for this concept and implies similar mechanistic roles of ST6GAL1 in TGF-β-induced EMT and cancer stem cells. Although these detailed mechanistic roles remain largely unknown, the current study clearly demonstrates the importance of ST6GAL1 in the sufficient induction of TGF-β-induced EMT and highlights the potential for targeting ST6GAL1 in clinical treatment.

Acknowledgments—We are grateful to Prof. K. Nagata and Dr. T. Kumagai (Tohoku Pharmaceutical University) for technical support for the Dual-Luciferase assay.

REFERENCES

1. Tarin, D., Thompson, E. W., and Newgreen, D. F. (2005) The fallacy of epithelial mesenchymal transition in neoplasia. *Cancer Res.* **65,** 5996–6000; discussion 6000–6001
2. Thiery, J. P., and Sleeman, J. P. (2006) Complex networks orchestrate epithelial-mesenchymal transitions. *Nat. Rev. Mol. Cell Biol.* **7,** 131–142
3. Greenburg, G., and Hay, E. D. (1982) Epithelia suspended in collagen gels can lose polarity and express characteristics of migrating mesenchymal cells. *J. Cell Biol.* **95,** 333–339
4. Hay, E. D. (1995) An overview of epithelio-mesenchymal transformation. *Acta Anat.* **154,** 8–20
5. Hugo, H., Ackland, M. L., Blick, T., Lawrence, M. G., Clements, J. A., Williams, E. D., and Thompson, E. W. (2007) Epithelial-mesenchymal and mesenchymal-epithelial transitions in carcinoma progression. *J. Cell. Physiol.* **213,** 374–383
6. Roberts, A. B., and Wakefield, L. M. (2003) The two faces of transforming growth factor β in carcinogenesis. *Proc. Natl. Acad. Sci. U.S.A.* **100,** 8621–8623
7. Kalluri, R., and Weinberg, R. A. (2009) The basics of epithelial-mesenchymal transition. *J. Clin. Invest.* **119,** 1420–1428
8. Valcourt, U., Kowanetz, M., Niimi, H., Heldin, C. H., and Moustakas, A. (2005) TGF-β and the Smad signaling pathway support transcriptomic reprogramming during epithelial-mesenchymal cell transition. *Mol. Biol. Cell* **16,** 1987–2002
9. Derynck, R., and Zhang, Y. E. (2003) Smad-dependent and Smad-independent pathways in TGF-β family signalling. *Nature* **425,** 577–584
10. Wu, G., Chen, Y. G., Ozdamar, B., Gyuricza, C. A., Chong, P. A., Wrana, J. L., Massagué, J., and Shi, Y. (2000) Structural basis of Smad2 recognition by the Smad anchor for receptor activation. *Science* **287,** 92–97
11. Maupin, K. A., Sinha, A., Eugster, E., Miller, J., Ross, J., Paulino, V., Keshamouni, V. G., Tran, N., Berens, M., Webb, C., and Haab, B. B. (2010) Glycogene expression alterations associated with pancreatic cancer epithelial-mesenchymal transition in complementary model systems. *PLoS One* **5,** e13002
12. Tan, Z., Lu, W., Li, X., Yang, G., Guo, J., Yu, H., Li, Z., and Guan, F. (2014) Altered *N*-glycan expression profile in epithelial-to-mesenchymal transition of NMuMG cells revealed by an integrated strategy using mass spectrometry and glycogene and lectin microarray analysis. *J. Proteome Res.* **13,** 2783–2795
13. Li, S., Mo, C., Peng, Q., Kang, X., Sun, C., Jiang, K., Huang, L., Lu, Y., Sui, J., Qin, X., and Liu, Y. (2013) Cell surface glycan alterations in epithelial mesenchymal transition process of Huh7 hepatocellular carcinoma cell. *PLoS One* **8,** e71273
14. Swindall, A. F., and Bellis, S. L. (2011) Sialylation of the Fas death receptor by ST6Gal-I provides protection against Fas-mediated apoptosis in colon carcinoma cells. *J. Biol. Chem.* **286,** 22982–22990

15. Liu, Z., Swindall, A. F., Kesterson, R. A., Schoeb, T. R., Bullard, D. C., and Bellis, S. L. (2011) ST6Gal-I regulates macrophage apoptosis via α2–6 sialylation of the TNFR1 death receptor. *J. Biol. Chem.* **286,** 39654–39662
16. Crespo, H. J., Cabral, M. G., Teixeira, A. V., Lau, J. T., Trindade, H., and Videira, P. A. (2009) Effect of sialic acid loss on dendritic cell maturation. *Immunology* **128,** e621–e631
17. Taniguchi, A., Higai, K., Hasegawa, Y., Utsumi, K., and Matsumoto, K. (1998) Differentiation elicits negative regulation of human β-galactoside α2,6-sialyltransferase at the mRNA level in the HL-60 cell line. *FEBS Lett.* **441,** 191–194
18. Büll, C., Boltje, T. J., Wassink, M., de Graaf, A. M., van Delft, F. L., den Brok, M. H., and Adema, G. J. (2013) Targeting aberrant sialylation in cancer cells using a fluorinated sialic acid analog impairs adhesion, migration, and *in vivo* tumor growth. *Mol. Cancer Ther.* **12,** 1935–1946
19. Seales, E. C., Jurado, G. A., Brunson, B. A., Wakefield, J. K., Frost, A. R., and Bellis, S. L. (2005) Hypersialylation of β1 integrins, observed in colon adenocarcinoma, may contribute to cancer progression by up-regulating cell motility. *Cancer Res.* **65,** 4645–4652
20. Xu, Q., Isaji, T., Lu, Y., Gu, W., Kondo, M., Fukuda, T., Du, Y., and Gu, J. (2012) Roles of *N*-acetylglucosaminyltransferase III in epithelial-to-mesenchymal transition induced by transforming growth factor β1 (TGF-β1) in epithelial cell lines. *J. Biol. Chem.* **287,** 16563–16574
21. Isaji, T., Im, S., Gu, W., Wang, Y., Hang, Q., Lu, J., Fukuda, T., Hashii, N., Takakura, D., Kawasaki, N., Miyoshi, H., and Gu, J. (2014) An oncogenic protein Golgi phosphoprotein 3 up-regulates cell migration via sialylation. *J. Biol. Chem.* **289,** 20694–20705
22. Ranjan, A., and Kalraiya, R. D. (2013) α2,6 sialylation associated with increased β1,6-branched *N*-oligosaccharides influences cellular adhesion and invasion. *J. Biosci.* **38,** 867–876
23. Jungert, K., Buck, A., von Wichert, G., Adler, G., König, A., Buchholz, M., Gress, T. M., and Ellenrieder, V. (2007) Sp1 is required for transforming growth factor-β-induced mesenchymal transition and migration in pancreatic cancer cells. *Cancer Res.* **67,** 1563–1570
24. Zhao, Y., Li, Y., Ma, H., Dong, W., Zhou, H., Song, X., Zhang, J., and Jia, L. (2014) Modification of sialylation mediates the invasive properties and chemosensitivity of human hepatocellular carcinoma. *Mol. Cell Proteomics* **13,** 520–536
25. Zheng, G., Lyons, J. G., Tan, T. K., Wang, Y., Hsu, T. T., Min, D., Succar, L., Rangan, G. K., Hu, M., Henderson, B. R., Alexander, S. I., and Harris, D. C. (2009) Disruption of E-cadherin by matrix metalloproteinase directly mediates epithelial-mesenchymal transition downstream of transforming growth factor-β1 in renal tubular epithelial cells. *Am. J. Pathol.* **175,** 580–591
26. Cha, S. K., Ortega, B., Kurosu, H., Rosenblatt, K. P., Kuro-O, M., and Huang, C. L. (2008) Removal of sialic acid involving Klotho causes cell-surface retention of TRPV5 channel via binding to galectin-1. *Proc. Natl. Acad. Sci. U.S.A.* **105,** 9805–9810
27. Kitazume, S., Imamaki, R., Ogawa, K., Komi, Y., Futakawa, S., Kojima, S., Hashimoto, Y., Marth, J. D., Paulson, J. C., and Taniguchi, N. (2010) α2,6-Sialic acid on platelet endothelial cell adhesion molecule (PECAM) regulates its homophilic interactions and downstream antiapoptotic signaling. *J. Biol. Chem.* **285,** 6515–6521
28. Zhu, Y., Srivatana, U., Ullah, A., Gagneja, H., Berenson, C. S., and Lance, P. (2001) Suppression of a sialyltransferase by antisense DNA reduces invasiveness of human colon cancer cells *in vitro*. *Biochim. Biophys. Acta* **1536,** 148–160
29. Lin, S., Kemmner, W., Grigull, S., and Schlag, P. M. (2002) Cell surface α2,6 sialylation affects adhesion of breast carcinoma cells. *Exp. Cell Res.* **276,** 101–110
30. Partridge, E. A., Le Roy, C., Di Guglielmo, G. M., Pawling, J., Cheung, P., Granovsky, M., Nabi, I. R., Wrana, J. L., and Dennis, J. W. (2004) Regulation of cytokine receptors by Golgi *N*-glycan processing and endocytosis. *Science* **306,** 120–124
31. de Oliveira, J. T., de Matos, A. J., Santos, A. L., Pinto, R., Gomes, J., Hespanhol, V., Chammas, R., Manninen, A., Bernardes, E. S., Albuquerque Reis, C., Rutteman, G., and Gärtner, F. (2011) Sialylation regulates galectin-3/ligand interplay during mammary tumour progression: a case of targeted uncloaking. *Int. J. Dev. Biol.* **55,** 823–834
32. Zhuo, Y., Chammas, R., and Bellis, S. L. (2008) Sialylation of β1 integrins blocks cell adhesion to galectin-3 and protects cells against galectin-3-induced apoptosis. *J. Biol. Chem.* **283,** 22177–22185
33. Zhuo, Y., and Bellis, S. L. (2011) Emerging role of α2,6-sialic acid as a negative regulator of galectin binding and function. *J. Biol. Chem.* **286,** 5935–5941
34. Lee, M., Lee, H. J., Bae, S., and Lee, Y. S. (2008) Protein sialylation by sialyltransferase involves radiation resistance. *Mol Cancer Res.* **6,** 1316–1325
35. Ma, H., Zhou, H., Song, X., Shi, S., Zhang, J., and Jia, L. (2014) Modification of sialylation is associated with multidrug resistance in human acute myeloid leukemia. *Oncogene* 10.1038/onc.2014.7
36. Bae, G. Y., Choi, S. J., Lee, J. S., Jo, J., Lee, J., Kim, J., and Cha, H. J. (2013) Loss of E-cadherin activates EGFR-MEK/ERK signaling, which promotes invasion via the ZEB1/MMP2 axis in non-small cell lung cancer. *Oncotarget* **4,** 2512–2522
37. Bakin, A. V., Tomlinson, A. K., Bhowmick, N. A., Moses, H. L., and Arteaga, C. L. (2000) Phosphatidylinositol 3-kinase function is required for transforming growth factor β-mediated epithelial to mesenchymal transition and cell migration. *J. Biol. Chem.* **275,** 36803–36810
38. Kattla, J. J., Carew, R. M., Heljic, M., Godson, C., and Brazil, D. P. (2008) Protein kinase B/Akt activity is involved in renal TGF-β1-driven epithelial-mesenchymal transition *in vitro* and *in vivo*. *Am. J. Physiol. Renal Physiol* **295,** F215–F225
39. Christie, D. R., Shaikh, F. M., Lucas, J. A., 4th, Lucas, J. A., 3rd, and Bellis, S. L. (2008) ST6Gal-I expression in ovarian cancer cells promotes an invasive phenotype by altering integrin glycosylation and function. *J. Ovarian Res.* **1,** 3
40. Shaikh, F. M., Seales, E. C., Clem, W. C., Hennessy, K. M., Zhuo, Y., and Bellis, S. L. (2008) Tumor cell migration and invasion are regulated by expression of variant integrin glycoforms. *Exp. Cell Res.* **314,** 2941–2950
41. Chen, Q., Manning, C. D., Millar, H., McCabe, F. L., Ferrante, C., Sharp, C., Shahied-Arruda, L., Doshi, P., Nakada, M. T., and Anderson, G. M. (2008) CNTO 95, a fully human anti αv integrin antibody, inhibits cell signaling, migration, invasion, and spontaneous metastasis of human breast cancer cells. *Clin. Exp. Metastasis* **25,** 139–148
42. Thomas, G. J., Lewis, M. P., Hart, I. R., Marshall, J. F., and Speight, P. M. (2001) αVβ6 integrin promotes invasion of squamous carcinoma cells through up-regulation of matrix metalloproteinase-9. *Int. J. Cancer* **92,** 641–650
43. Thomas, G. J., Lewis, M. P., Whawell, S. A., Russell, A., Sheppard, D., Hart, I. R., Speight, P. M., and Marshall, J. F. (2001) Expression of the alphavbeta6 integrin promotes migration and invasion in squamous carcinoma cells. *J. Invest. Dermatol.* **117,** 67–73
44. Sloan, E. K., Pouliot, N., Stanley, K. L., Chia, J., Moseley, J. M., Hards, D. K., and Anderson, R. L. (2006) Tumor-specific expression of αvβ3 integrin promotes spontaneous metastasis of breast cancer to bone. *Breast Cancer Res.* **8,** R20
45. Mamuya, F. A., and Duncan, M. K. (2012) aV integrins and TGF-β-induced EMT: a circle of regulation. *J. Cell Mol. Med.* **16,** 445–455
46. Hinek, A., Bodnaruk, T. D., Bunda, S., Wang, Y., and Liu, K. (2008) Neuraminidase-1, a subunit of the cell surface elastin receptor, desialylates and functionally inactivates adjacent receptors interacting with the mitogenic growth factors PDGF-BB and IGF-2. *Am. J. Pathol.* **173,** 1042–1056
47. Lillehoj, E. P., Hyun, S. W., Feng, C., Zhang, L., Liu, A., Guang, W., Nguyen, C., Luzina, I. G., Atamas, S. P., Passaniti, A., Twaddell, W. S., Puché, A. C., Wang, L. X., Cross, A. S., and Goldblum, S. E. (2012) NEU1 sialidase expressed in human airway epithelia regulates epidermal growth factor receptor (EGFR) and MUC1 protein signaling. *J. Biol. Chem.* **287,** 8214–8231
48. Shen, L., Qu, X., Ma, Y., Zheng, J., Chu, D., Liu, B., Li, X., Wang, M., Xu, C., Liu, N., Yao, L., and Zhang, J. (2014) Tumor suppressor NDRG2 tips the balance of oncogenic TGF-β via EMT inhibition in colorectal cancer. *Oncogenesis* **3,** e86
49. Taniguchi, A., Hasegawa, Y., Higai, K., and Matsumoto, K. (2000) Transcriptional regulation of human β-galactoside α2, 6-sialyltransferase (hST6Gal I) gene during differentiation of the HL-60 cell line. *Glycobiology* **10,** 623–628

50. Gu, J., Nishikawa, A., Tsuruoka, N., Ohno, M., Yamaguchi, N., Kangawa, K., and Taniguchi, N. (1993) Purification and characterization of UDP-*N*-acetylglucosamine: α-6-D-mannoside β 1–6*N*-acetylglucosaminyltransferase (*N*-acetylglucosaminyltransferase V) from a human lung cancer cell line. *J. Biochem.* **113,** 614–619
51. Schachter, H. (1986) Biosynthetic controls that determine the branching and microheterogeneity of protein-bound oligosaccharides. *Adv. Exp. Med. Biol.* **205,** 53–85
52. Schachter, H., Narasimhan, S., Gleeson, P., and Vella, G. (1983) Control of branching during the biosynthesis of asparagine-linked oligosaccharides. *Can. J. Biochem. Cell Biol.* **61,** 1049–1066
53. Pinho, S. S., Osório, H., Nita-Lazar, M., Gomes, J., Lopes, C., Gärtner, F., and Reis, C. A. (2009) Role of E-cadherin *N*-glycosylation profile in a mammary tumor model. *Biochem. Biophys. Res. Commun.* **379,** 1091–1096
54. Saldova, R., Piccard, H., Pérez-Garay, M., Harvey, D. J., Struwe, W. B., Galligan, M. C., Berghmans, N., Madden, S. F., Peracaula, R., Opdenakker, G., and Rudd, P. M. (2013) Increase in sialylation and branching in the mouse serum *N*-glycome correlates with inflammation and ovarian tumour progression. *PLoS One* **8,** e71159
55. Granovsky, M., Fata, J., Pawling, J., Muller, W. J., Khokha, R., and Dennis, J. W. (2000) Suppression of tumor growth and metastasis in Mgat5-deficient mice. *Nat. Med.* **6,** 306–312
56. Zhang, Z., Sun, J., Hao, L., Liu, C., Ma, H., and Jia, L. (2013) Modification of glycosylation mediates the invasive properties of murine hepatocarcinoma cell lines to lymph nodes. *PLoS One* **8,** e65218
57. Woodard-Grice, A. V., McBrayer, A. C., Wakefield, J. K., Zhuo, Y., and Bellis, S. L. (2008) Proteolytic shedding of ST6Gal-I by BACE1 regulates the glycosylation and function of α4β1 integrins. *J. Biol. Chem.* **283,** 26364–26373
58. Amano, M., Galvan, M., He, J., and Baum, L. G. (2003) The ST6Gal I sialyltransferase selectively modifies *N*-glycans on CD45 to negatively regulate galectin-1-induced CD45 clustering, phosphatase modulation, and T cell death. *J. Biol. Chem.* **278,** 7469–7475
59. Liu, Y. C., Yen, H. Y., Chen, C. Y., Chen, C. H., Cheng, P. F., Juan, Y. H., Chen, C. H., Khoo, K. H., Yu, C. J., Yang, P. C., Hsu, T. L., and Wong, C. H. (2011) Sialylation and fucosylation of epidermal growth factor receptor suppress its dimerization and activation in lung cancer cells. *Proc. Natl. Acad. Sci. U.S.A.* **108,** 11332–11337
60. Meng, L., Forouhar, F., Thieker, D., Gao, Z., Ramiah, A., Moniz, H., Xiang, Y., Seetharaman, J., Milaninia, S., Su, M., Bridger, R., Veillon, L., Azadi, P., Kornhaber, G., Wells, L., Montelione, G. T., Woods, R. J., Tong, L., and Moremen, K. W. (2013) Enzymatic basis for *N*-glycan sialylation: structure of rat α2,6-sialyltransferase (ST6GAL1) reveals conserved and unique features for glycan sialylation. *J. Biol. Chem.* **288,** 34680–34698
61. Swindall, A. F., Londoño-Joshi, A. I., Schultz, M. J., Fineberg, N., Buchsbaum, D. J., and Bellis, S. L. (2013) ST6Gal-I protein expression is upregulated in human epithelial tumors and correlates with stem cell markers in normal tissues and colon cancer cell lines. *Cancer Res.* **73,** 2368–2378
62. Mani, S. A., Guo, W., Liao, M. J., Eaton, E. N., Ayyanan, A., Zhou, A. Y., Brooks, M., Reinhard, F., Zhang, C. C., Shipitsin, M., Campbell, L. L., Polyak, K., Brisken, C., Yang, J., and Weinberg, R. A. (2008) The epithelial-mesenchymal transition generates cells with properties of stem cells. *Cell* **133,** 704–715